

On-Orbit Demonstration of the Space Weather and Meteor Impact Monitoring Network

Victor Hernandez¹, Aaditya Ravindran²

¹School of Earth and Space Exploration, ²School of Electrical, Computer and Energy Engineering,
Arizona State University
781 E Terrace Mall, 480-727-2136, vaherna4@asu.edu

Faculty Advisors: Erik Asphaug, Jekan Thangavelautham
School of Earth and Space Exploration, Arizona State University

ABSTRACT

Incidents like the Chelyabinsk meteor airburst in 2013 show the potential dangers of a meteor impact on modern human civilization. However, not much is known about meteor impacts, including frequency of high impact bursts, typical size and composition. We propose the development of a Space Weather and Meteor Impact Monitoring Network (SWIMNet). SWIMNet will be composed of two observer CubeSats located in Low Earth Orbit (LEO) to autonomously detect and track meteor trails in the Earth's atmosphere. A third CubeSat will contain a 2 kg meteorite that will be deployed on an Earth reentry trajectory. The observer satellites, combined with ground telescopes will track this artificial reentry event and be used to validate the autonomous detection and tracking algorithms. Beyond this demonstration, the observer satellites will operate in Earth orbit for up to 1 year and detect natural meteor trails. The proposed mission utilizes off-the-shelf CubeSat technology and points towards a feasible pathway for further development.

INTRODUCTION

Meteors are the remnants of asteroids that are pulled in by Earth's gravity towards a fiery impact. These objects, depending on their composition enter through the Earth's atmosphere and can cause explosions of several kilotons to hundreds of megatons. A major recent incident was the Chelyabinsk meteor airburst in 2013 (Figure 1) [1, 3, 5]. The Chelyabinsk meteor was 20 meters in diameter with a kinetic energy of 400-500 kT at 30 km air burst height, about 26 times the energy of the Hiroshima atomic bomb [3]

Meteor impact events have been known to cause largescale extinction events including the dinosaur-killing Chicxulub event. Current theories about meteor entry and impact events need to be verified for us to better prepare for the next "big one." This requires improved understanding of meteor entry into the Earth's atmosphere and efforts to better monitor them to provide timely warnings. There lacks a dedicated satellite network to observe and characterize meteor impacts in the upper atmosphere. Such a network is critical towards making predictions and timely warning of incoming meteor impact dangers.

Only partial, filtered data is publicly available to the scientific community. There is an immediate need for a network capable of distributing raw findings for a more complete understanding of these events. To achieve this, a satellite would require a camera capable of

operating in the visible spectrum to detect and track the meteor fireball and dust-ion tail upon reentry, which lasts in duration from seconds to hours (Figure 2).



Figure 1: Chelyabinsk Meteor Trail captured from the ground in 2013.

Detection capabilities of this nature have already been proven by Doppler weather radar; however, an onboard algorithm will have to be optimized for space observations [4]. Dedicated observations over time will increase confidence in frequency of events as a function of size and energy and physical characteristics of meteor mappings. Meteor trajectories can also be used to reconstruct the original orbits, a task that is made difficult without adequate observation data, to construct more accurate predictive orbital models used in meteor mitigation analysis [1].

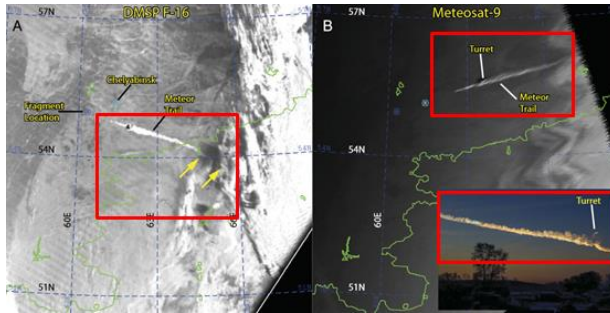


Figure 2: Earth-Viewing Satellite Perspectives and ground monitoring of the Chelyabinsk Meteor Event [5].

In this paper we propose development of a mission concept to demonstrate monitoring of meteor reentry events. The proposed mission concept is a major advancement from our earlier work from [2]. In this new mission concept, we outline a compelling pathway for validation of meteor detection and reentry in Low Earth Orbit. Our earlier mission concept required a GEO orbit and because those launch opportunities are limited, we have developed a revised mission concept. A sizable meteor reentry and impact event is rare and hence our mission concept includes plans for a controlled reentry of a meteor deployed from a spacecraft. In addition, several other spacecraft will monitor the meteor entering the Earth's atmosphere. Our work has identified CubeSats as the ideal low-cost platform to demonstrate this mission.

We propose to develop a pair of low-cost 3U (10 cm × 10 cm × 30 cm) Space Weather and Meteor Impact Monitoring Network (SWIMNet) to operate in Low Earth Orbit (LEO). Each satellite will require a visible imager to autonomously detect, image, and track meteor impacts into Earth's upper atmosphere using an onboard algorithm optimized for such observations [2]. Each imaging satellite is named an OSat (Observational Satellite) and will be accompanied by the RockSat (Rock Satellite), a 6U (36 cm × 24 cm × 12 cm) CubeSat carrying a meteor payload. SWIMNet's primary mission will take images of the RockSat reentry event using the OSats. After monitoring the meteor reentry from RockSat, the OSats will continue to monitor natural meteor reentry for several months.

Small platforms such as Aerospace Corporation's REBR [6] have been shown to successfully reenter the Earth's atmosphere and communicate the contents of a data recorder. A variant of REBR is available commercially and is called RED-Data2 [7]. In contrast, our RockSat doesn't have to successfully operate upon reentry and is intended to simply simulate reentry conditions, which imposes a lower threshold for

success. Furthermore, the reentering spacecraft will be monitored from space and the ground using telescopes. This combination of monitoring sources will provide different viewpoints and provide the mission team a better understanding of the operational challenges and limitations with the approach.

In the following sections, we will present a preliminary design of the proposed mission concept, followed by concept of operations, details on the subsystems, discussion and conclusions.

THE MISSION

The SWIMNet mission concept has one primary mission objective and that is to autonomously detect, image, and selectively downlink a meteor impact event or analogous event from a LEO satellite. A secondary objective is to track and image the same event using a ground telescope. A third objective is to perform characterization of the effects of drag upon reentry of objects into the upper atmosphere. The minimum success criterion for the mission requires detection and capturing of one image of the meteor reentry event and downlinking to ground using onboard algorithms. The full mission success criteria would require detection, tracking, and capturing of images of the event at 1 fps and downlinking to ground using an onboard algorithm.

A secondary mission success criterion will be to obtain ground truth of a meteor reentry event, followed by tracking of the event at 1 fps. Finally, a tertiary mission objective will be to capture and downlink satellite position data at known intervals for the RockSat.

As noted earlier, the proposed mission concept contains a RockSat (Rock Satellite), a 6U (36 cm × 24 cm × 12 cm) CubeSat carrying a meteor payload and two 3U OSats (Observational Satellites) to monitor RockSat and the meteor payload reentering Earth's atmosphere.

CONCEPT OF OPERATIONS

The concept of operations for the SWIMNet mission is shown in Figure 3. The Launch for the SWIMNet mission is anticipated in 2020 or 2021, depending on launch vehicle availability. Once the satellites reach the International Space Station (ISS), they will be stored onboard until they are ready for a timed deployment, starting with the OSats (Figure 4). Upon deployment, the satellites will undergo initial operations to stabilize and establish ground communications.

A period of 6 weeks will be given for commissioning of the satellites, including instrument calibration and testing. Once the satellites have been commissioned, the RockSat will initiate a propulsive maneuver to line

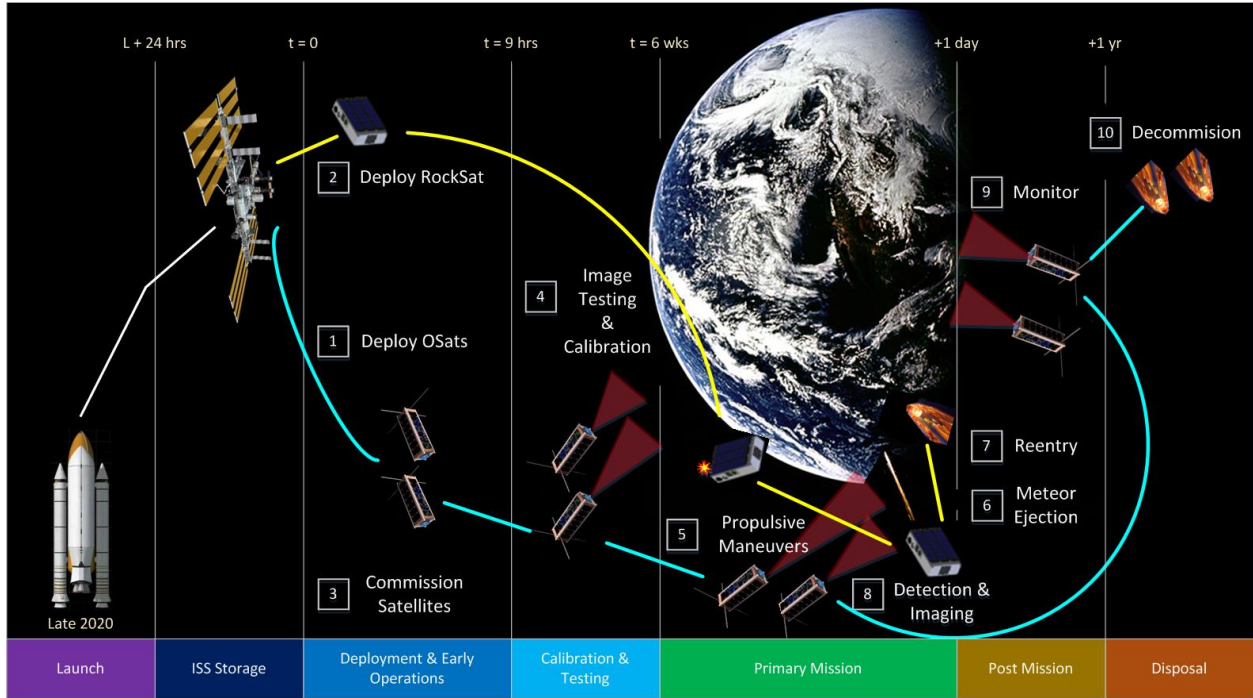


Figure 3: Concept of Operations for the Space Weather and Meteor Impact Monitoring Network (SWIMNet).

up with the OSats. The RockSat will then engage a propulsive maneuver towards the Earth’s upper atmosphere. RockSat will use nichrome wire burn wire to passively eject a meteor rock sample. OSat will detect and image the RockSat and meteor reentry event and downlink the data to ground station over several

passes. Two OSats are required to provide dedicated observation of the RockSat and meteor reentering the Earth’s atmosphere. The OSats will continue to monitor, detect, and image natural meteor reentry events for up to 1 year until they reenter Earth.

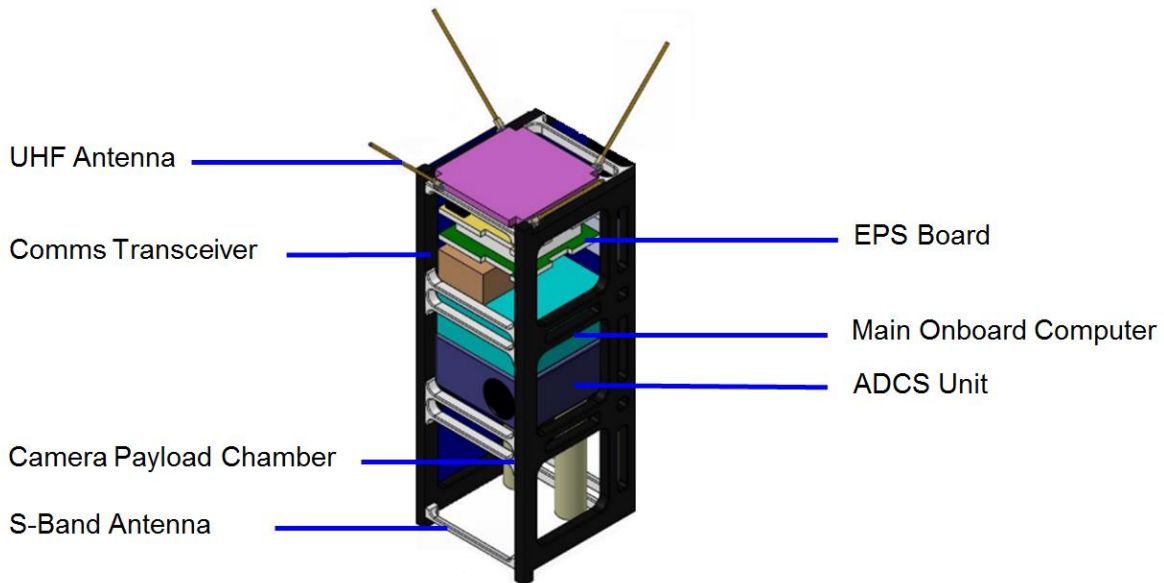


Figure 4: Observer Satellite (OSat).

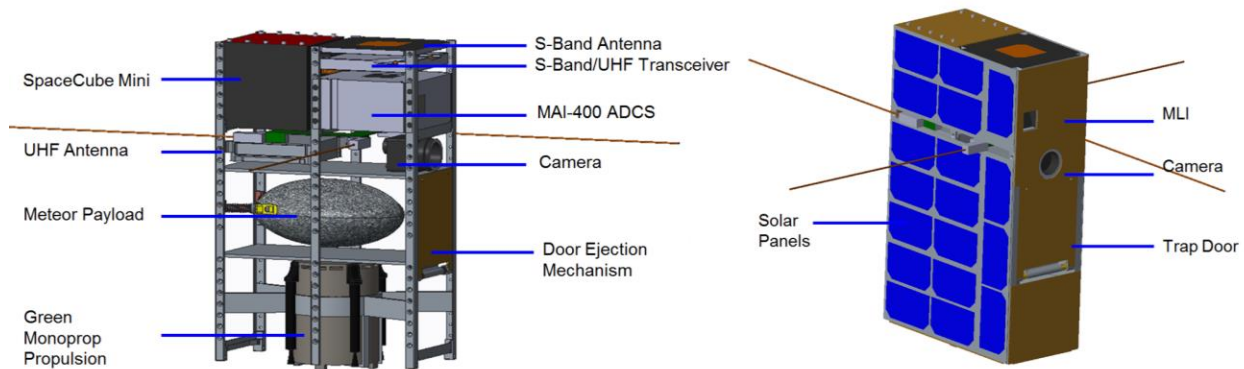


Figure 5: Rock Satellite (RockSat).

SPACECRAFTS

Figure 4 shows a preliminary design of an OSat. Figure 5 show a preliminary design of RockSat. The mass budgets for each OSat and RockSat are shown in Table 1 and Table 2 respectively.

Each OSat has a mass of 3.2 kg and with 15% component margin, the total mass is 3.8 kg. The OSat utilizes the Tyvak Endeavour 3U chassis, containing body mounted triple junction solar panels that provide 4 W (avg) in orbit. For the instruments subsystem, a camera was selected to meet the minimum success criteria for the primary mission and a ground telescope for the secondary mission. Position data collected by the ADCS and CDH modules sufficiently meet the success criteria for the tertiary mission objectives.

Table 1: Preliminary Mass Budget of Each Observation Satellite (OSat).

System	Mass (kg)	Margin	Total Mass (kg)
Communications	0.19	15%	0.22
Onboard CD&H, EPS	0.20	15%	0.23
Instrument - Camera	0.25	15%	0.29
Battery & Solar Panels	0.65	15%	0.75
Attitude Determination & Control	0.74	15%	0.85
Structure	1.10	15%	1.32
Thermal	0.10	15%	0.15
Total			3.8

Pointing accuracy for the camera will be handled by the ADCS subsystem using reaction wheels and magnetorquers. Data exchange between the satellite and ground station will utilize UHF and S-Band communications units. Figure 5 shows a preliminary

design of RockSat. RockSat has a mass of 9.2 kg with 1.4 kg contingency.

RockSat utilizes the Pumpkin Supernova 6U chassis, with body mounted solar panels providing 15 W average power. For the RockSat propulsion system, green monoprop was selected to meet delta-v requirements. Not shown are the satellite solar panels.

Table 2: Preliminary Mass Budget of Rock Satellite (RockSat).

System	Mass (kg)	Margin	Total Mass (kg)
Communications	0.19	15%	0.22
Onboard CD&H, EPS	0.20	15%	0.23
Instrument - Camera	0.07	15%	0.08
Battery & Solar Panels	0.73	15%	0.84
Attitude Determination & Control	0.74	15%	0.85
Structure	1.64	15%	1.88
Payload	2.00	15%	2.30
Thermal	0.10	15%	0.15
Propulsion	2.80	15%	3.22
Deployment	0.70	15%	0.81
Total			10.6

The following subsystems were selected for the OSat to meet mission requirements: Electrical Power System (EPS), Command and Data Handling (CDH), Altitude Determination and Control System (ADCS), Instruments, Thermal Control System (TCS), Communications (Comms), and Structures. For RockSat, all of these subsystems were selected with the addition of propulsion. The system architectures for OSat and RockSat are shown in Figure 6 and 7.

Both the OSat and RockSats are controlled by the SpaceCube Mini main onboard computer (MOBC). Communications for both satellites utilize an Endurosat UHF/S-Band Transceiver and S-Band patch antenna coupled with a Nanoavionics UHF antenna. EPS for both satellites will incorporate external solar panels with battery storage managed by the SpaceCube Mini EPS board. ADCS for both satellites will utilize the MAI-400 ADCS unit, a package of reaction wheels, magnetorquers, sun sensors, horizon sensors, and star trackers. OSat's payload consists of a Pentax B5014A lens attached to an e2V CIRES Ruby camera. RockSat's payload is a meteor rock sample.

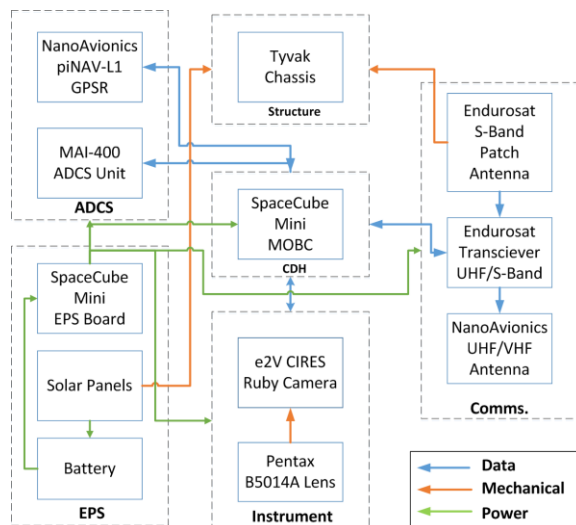


Figure 6: System architecture for the Observer Satellite (OSat).

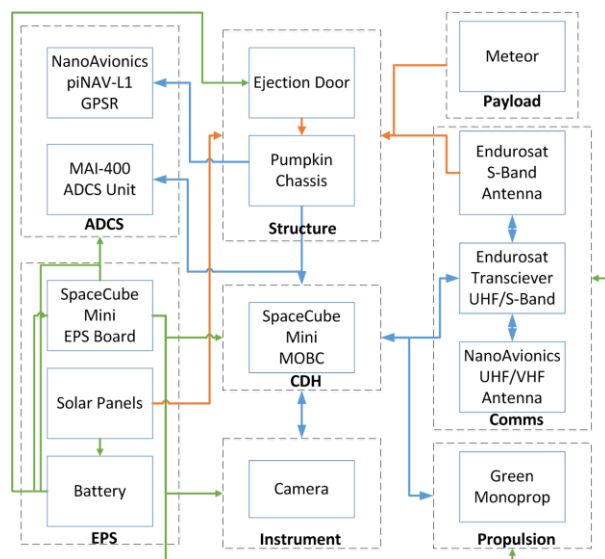


Figure 7: System architecture for the Rock Satellite (RockSat).

The meteor rock requires a mechanical mechanism for holding it in place during transport and for ejecting it during the reentry sequence.

ATTITUDE DETERMINATION AND CONTROL

The ADCS subsystem consists of two subsystems, namely, Attitude Determination System (ADS) and the Attitude Control System (ACS). The ADS is being designed to monitor angular velocity to a precision of $0.01^\circ/s$ on all axes and attitude with accuracy less than 0.01° . The OSats shall be able to accurately track the RockSat with a 1° half cone error. The attitude control system is expected to de-tumble the RockSat/OSat(s) to angular velocities under $0.2^\circ/sec$. For communication, the RockSat/OSat(s) body axes shall be pointed under a 1° half cone error. For RockSat, propulsion requires a thrust vector under a 1° half cone error.

Based on these requirements, an ADCS trade study was done and MAI-400 by Maryland Aerospace (See Figure 8) was found to have the best trade-off between cost and pointing accuracy. The specifications for the MAI-400 is shown in Table 3. A GPS system selected for position tracking was piNAV-L1 by Nano avionics.

Table 3: ADCS Specifications

Specification	MAI-400
Mass	0.694 kg
Dimension	10 x 10 x 5.16 cm
Power (Nominal)	1.13 W
Power (Max torque)	2.05 W
Magnetic Dipole Moment	0.108 Am ²
Pointing Accuracy	$\ll 1^\circ$
Momentum Storage	11.076 mNm
Max Torque	0.64 mNm
Reaction Wheel Stability	< 0.2 arcsec

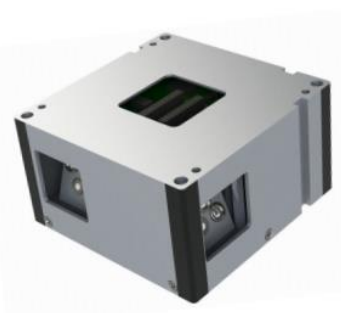


Figure 8: MAI-400 ADCS

The architecture of the ADCS system for RockSat and OSat is shown in Figure 9 and 10 respectively. The

MAI-400 can be ordered with the required sensors and actuators. The MAI-400 and the GPS module (piNav-L1) connect to the Command and Data Handling system through the Onboard computer (OBC). The difference between the RockSat and OSat architecture is that the RockSat will have an accelerometer, to measure the deceleration while reentering and the OSat will not.

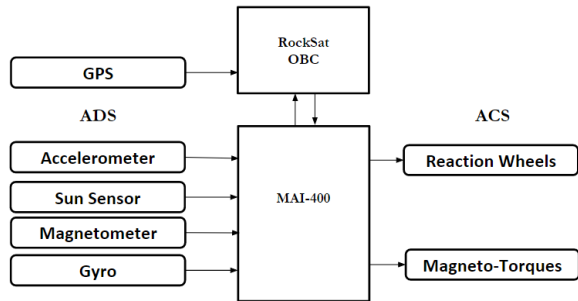


Figure 9: RockSat ADCS architecture

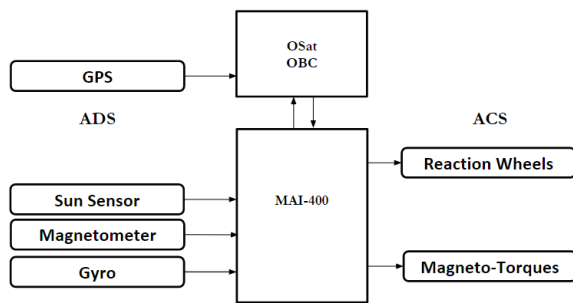


Figure 10: OSat ADCS architecture

The RockSat/OSat(s) will have 3 modes of operation,

1. Detumble - post deployment
2. Communication – pointing to Earth
3. Thrust vector for the RockSat – align the thrust vector to lower the altitude
4. Scan mode for the OSat – points the camera towards the RockSat.

The control strategy for the satellites is summarized in Figure 11 and uses conventional techniques to achieve the required attitude control.

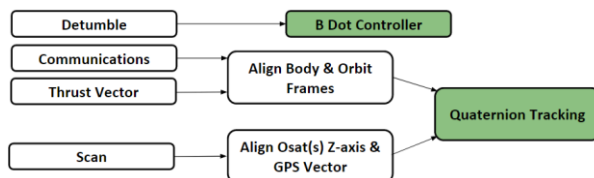


Figure 11: Attitude Control Strategies

Simulations were conducted to analyze the initial feasibility of the approach using Matlab and STK. The desaturation times for the detumble mode are shown in Table 4. The simulation parameters considered that the RockSat has more mass than the OSat which is why the RockSat takes more time to detumble.

Table 4: Detumbling times

Initial Spin Rates	RockSat	OSat
5°/s	2.74 hrs	1.14 hrs
10°/s	3.46 hrs	1.16 hrs
15°/s	3.61 hrs	1.21 hrs

The simulation results that thrust vector pointing and communication mode pointing (Figure 12 and 13) can be achieved in about one or two minutes, depending on the initial conditions (after detumbling).

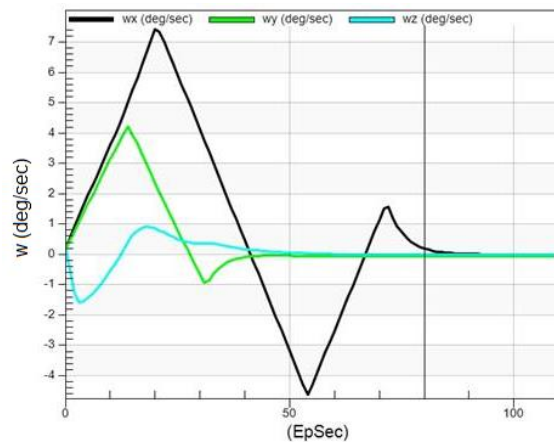


Figure 12: Thrust Vectoring Mode (angular velocity).

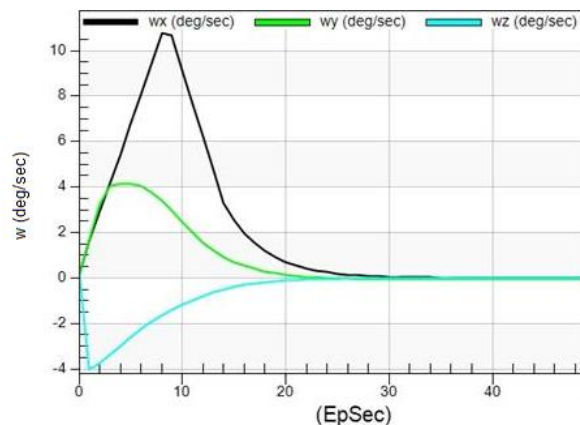


Figure 13: Communication pointing mode (angular velocity).

PROPULSION SUBSYSTEM

The propulsion subsystem for the RockSat is designed to provide a delta-v of 110 m/s and a total impulse of 785 Ns. The subsystem is expected to operate using less than 15 W of power. In addition, the pressure inside the propulsion tanks will be under 25 bar. The propulsion technology was selected according to the trade study shown in Table 5.

Table 5: Propulsion Technology Trade Study

Parameter/ Technology	Green Mono.	Cold Gas	Elec. Prop	Hydrazine
Thrust	High	Low	Very Low	High
Isp	High	Low	Very High	High
Safety	High	High	High	Low
Simplicity	Moderate	Moderate	High	Moderate
Cost	High	Moderate	High	Moderate

The selected propulsion technology is Green Monopropellant. This type of propulsion possesses high density and increased maneuverability compared to Hydrazine. In addition, its low toxicity, fewer handling restrictions and complexity makes it a very compelling option. The lower freezing point decreases the power requirement to maintain temperature. There is currently a proof of technology mission that is scheduled to fly in 2017, called the NASA Green Monopropellant Infusion Mission. CubeSat Green Monopropellant Thrusters are in continued development at several competing companies including Vacco, Aerojet, Busek and CU Aerospace.

The proposed Green Monopropellant propulsion system is the MPS-130 from Aerojet. Its mean performance characteristics can be seen in Figure 14:



Figure 14: MPS-130 from Aerojet

Maneuver Overview

After the CubeSats have been deployed from ISS and have gone through check out and calibration phase, two maneuvers will be conducted by RockSat (Figure 15).

The rendezvous maneuver with the two Observer Satellites will consist of reducing the perigee to an altitude of 250 km. This maneuver will require a ΔV of 43 m/s. The final maneuver will force the atmospheric entry of the RockSat and will require a ΔV of 53 m/s. The remaining ΔV of 15 m/s serves as margin.

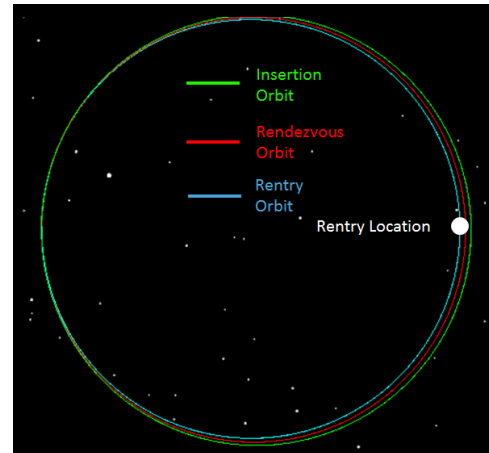


Figure 15: SWIMSat Orbital Maneuvers

COMMUNICATION SUBSYSTEMS

The communication subsystem on the OSats and RockSat shall be capable of sending beacons, images, housekeeping, and telemetry data to the Ground Station using UHF and S-band. For our system design, we have included minimum of 6 dB margin in the telecommunications link analysis for both the uplink and the downlink.

The communication subsystem architecture is shown in Figure 16. The communication subsystem consists of the transceiver, S-band and UHF band antennas, and a microcontroller. The EPS powers the microcontroller and the transceiver (Figure 17). The transceiver is responsible for low noise amplification using a low noise amplifier (LNA), demodulating the signal at the receiver end, and modulating, then amplifying, in the transmitting end. The microcontroller takes care of encoding and decoding the signal if the transceiver does not have this capability. The signal is sent/received by the CDH onboard computer through an SPI or I2C interface.

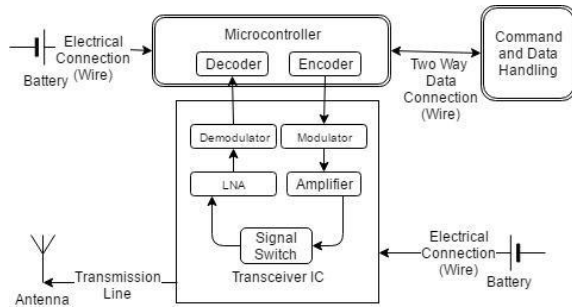


Figure 16: Communication system architecture



Figure 17: Endurosat S/UHF band transceiver

A trade study on transceivers was conducted and the Endurosat S/UHF band transceiver (See Figure 17) was found to have the best tradeoff between sensitivity, power amplifier efficiency, and transmit power. Hence, four possibilities are discussed for the link budget analysis:

1. UHF band uplink and S-band downlink
2. S-band uplink and UHF band downlink
3. UHF band uplink and downlink
4. S-band uplink and downlink

The advantage of having an S-band downlink is higher data rate. The link budget is summarized in Table 6. It will be shown later that the link budget satisfies the mission requirements.

Table 6: Link Budget Summary

A: UHF band uplink, S-band downlink

Parameter	Uplink Value	Downlink Value	Units
Antenna Gain	14.1	6.0	dBi
Terminal EIRP	20.5	6.5	dBW
Ground station pointing loss	5.7	14.4	dB
Path loss	154.2	169.0	dB
Isotropic signal at Spacecraft	-137.8	-164.9	dBW
System Desired Data Rate	9.6	16.0	kbps
System Link Margin	10.0	7.6	dB

B: S-band uplink, UHF band downlink

Parameter	Uplink Value	Downlink Value	Units
Antenna Gain	35.4	2.0	dBi
Terminal EIRP	41.8	2.8	dBW
Ground station pointing loss	14.4	5.7	dB
Path loss	169.0	154.1	dB
Isotropic signal level at Spacecraft	-148.4	-150.4	dBW
System Desired Data Rate	16.0	9.6	kbps
System Link Margin	7.0	10.6	dB

C: UHF band uplink, UHF band downlink

Parameter	Uplink Value	Downlink Value	Units
Antenna Gain	14.1	2.0	dBi
Terminal EIRP	20.5	2.8	dBW
Ground station pointing loss	5.7	5.7	dB
Path loss	154.2	154.1	dB
Isotropic signal level at Spacecraft	-135.5	-150.7	dBW
System Desired Data Rate	9.6	9.6	kbps
System Link Margin	11.9	6.0	dB

D: S-band uplink, S-band downlink

Parameter	Uplink Value	Downlink Value	Units
Antenna Gain	35.0	6.0	dBi
Terminal EIRP	46.5	2.8	dBW
Ground station pointing loss	24.4	14.4	dB
Path loss	169.0	169.0	dB
Isotropic signal level at Spacecraft	-139.4	-168.6	dBW
System Desired Data Rate	16.0	16.0	kbps
System Link Margin	7.7	7.6	dB

POWER SUBSYSTEM

The EPS for OSat and RockSat will be responsible for supplying all other subsystems with the required voltages and current. In order to sustain operation, the EPS will use solar panels to charge the batteries and maintain a minimum power level. Figure 18 shows the basic structure of the EPS.

The major components of the EPS for each satellite will consist of batteries for energy storage, regulators to reduce the battery voltage to the supply voltages required by the subsystems, solar panels for recharging the batteries, and cabling to distribute the power throughout the satellite.

The batteries selected for the SWIMNet mission include the GOMspace NanoPower BPX and BP4. RockSat will be powered by the NanoPower BPX, consisting of lithium ion cells with a total capacity of 77 watt hours (Wh). The less power intensive OSat will use the NanoPower BP4 battery, which consists of 4 lithium ion cells with a total capacity of 38.5 Wh.

To complement the battery selection, the GOMspace NanoPower P31uX power supply has been chosen for the best compatibility and ease of integration. The NanoPower P31uX consists of 5 outputs configurable to 3.3 V or 5 V and 0.5 A to 2.5 A current limits. This configuration is well suited to the SWIMNet mission as all selected components operate on either 3.3 V or 5 V and are within the current sourcing capabilities of the P31uX.

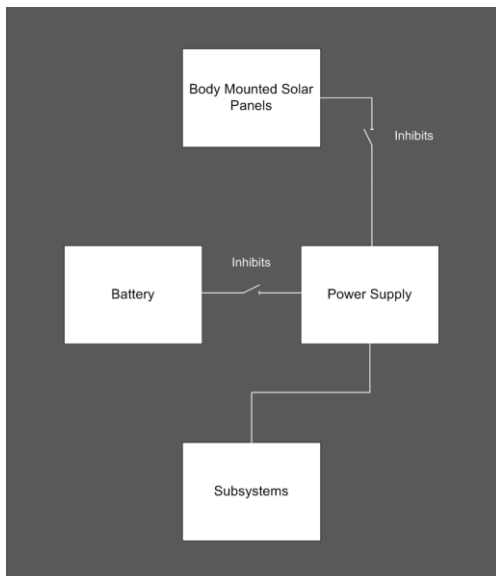


Figure 18: Electrical Power Subsystem Architecture for OSat & RockSat.

Solar panels for both RockSat and OSat will be body mounted triple junctions cells from Emcore. Initial simulations of power generation show Rocksat capable of producing up to 20 W, and OSat capable of producing up to 10 W.

The current power budget estimates that RockSat will dissipate an average of 16 W across all modes of operation while OSat has an average of 9 W. Given the estimated power production from the solar panels, RockSat and OSat will have positive power budgets for much of their operation. Additionally, if further simulations suggest that more power is necessary, adding deployable solar arrays is an option.

All power cabling used will be of an appropriate gauge for the voltage and current it will carry. All power wiring will have shielding and be routed in such a manner to minimize electromagnetic interference (EMI).

COMMAND, DATA HANDLING AND SOFTWARE SUBSYSTEM

The CDH system requirements are summarized in Table 7. Performance, power, size, and memory are the major design constraints.

Table 7: CDH Requirements

Parameter	Requirements
CPU Frequency	> 400 MHz
Power	< 10 W
Data Storage	> 32 GB
Interfaces	Shall provide support for high speed devices
Fault Tolerance	Device level fault tolerant support
Event Scheduling	Priority based event handling for event scheduling

A trade study was conducted and it was found that SpaceCube Mini [8], originally developed by NASA Goddard and now commercialized by Cobham-Aeroflex (See Figure 19), met the requirements of the SWIMNet mission concept. Some important features of the SpaceCube Mini are shown below:

- 512 M x 16 of SDRAM
- 96 gigabits of FLASH
- 12 bit analog to digital converter
- Local power regulation
- 4 Spacewire or 8 LVDS interfaces
- 8 RS422 interfaces
- Xilinx Multi-Gigabit Transceiver (MGT)



Figure 19: SpaceCube MINI folded flat

The SpaceCube Mini consists of 3 main components (as shown in Figure 20):

- The processor card – as the name suggests, the card consisting of the main FPGA processor along with the main interfaces
- The hybrid card – which consists of the Aeroflux FPGA which is interfaced with the camera module.
- The power card – which is responsible for supplying appropriate amount of power to the rest of the board and some components.

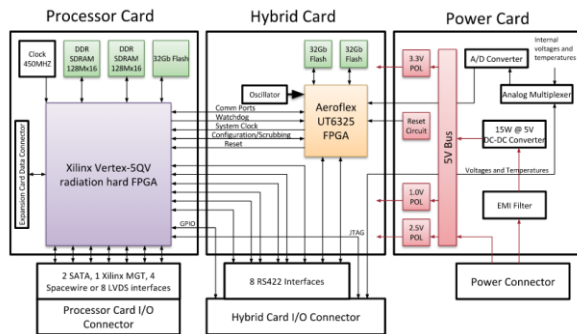


Figure 20: SpaceCube Mini architecture

All of the peripherals connect to the SpaceCube Mini through the RS422/LVDS interface. These include the communication module, GPRS, EPS module, ADCS module, thermal modules, and the camera module in the OSat(s) and RockSat. In addition to the previously mentioned modules, RockSat also has a propulsion system and the meteor release mechanism connected to the OBC.

The software architecture of the OSat and RockSat can be found in Figure 21 and 22. The OBC is responsible for data logging, maintenance, interfacing the ADCS, Communications, EPS, and the camera in both the OSat and RockSat. Additionally in RockSat, the OBC is responsible for propulsion and rock release mechanism.

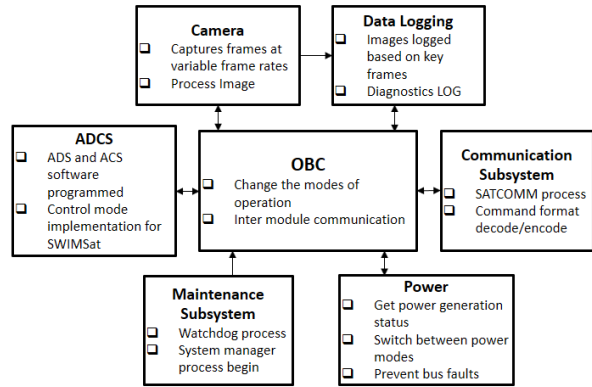


Figure 21: OSat Software architecture

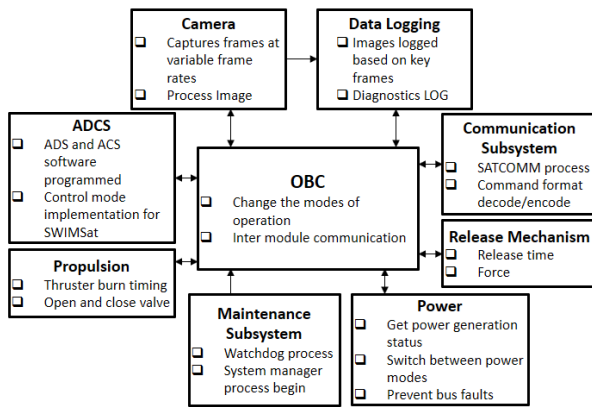


Figure 22: RockSat Software architecture

The CDH system is responsible for the following operating modes: (1) deployment, (2) detumble, (3) communication data, (4) query beacon, (5) attitude determination and control, (6) propulsion/thrusting (on RockSat), and (7) reentry track mode (on OSat).

Table 8 shows the amount of data which can be received/transmitted per orbit, which corresponds to the data budget of the primary mission. Similar calculations were made for other modes and the total data was found to be around 250 to 500 kbits for other modes in downlink and 45 to 200 kbits for uplink.

Table 8: RockSat Primary Mission data per orbit

Parameter	Downlink Value	Uplink Value
Sample size (bits)	717,767	476
Sample overhead (bits)	192	48
Frequency (sample/sec)	1.15	1
Duration (sec)	16,260	300
Sample total (bits)	43,421,940	157,200
Downlink overhead (bits)	3,618,495	13,100
Total (bits)	47,040,435	170,300

Table 9: OSat Primary Mission data per orbit

Parameter	Downlink	Uplink
Sample size (bits)	2,082,084	476
Sample overhead (bits)	192	48
Frequency (sample/sec)	1.15	1
Duration (sec)	16,260	300
Sample total (bits)	1,248,824,400	157,200
Downlink overhead (bits)	104,068,700	13,100
Total (bits)	1,352,893,100	170,300

The OSat will run a meteor detection algorithm to track the RockSat upon reentry. The meteor detection algorithm works by detecting trails from a ratio of length to height after thresholding the image. Once a trail is detected, the algorithm then proceeds to detect and label different ‘blobs’ of the meteor. Finally, the number of blobs are counted and thresholded to a certain brightness. Figure 23 and 24 show early testing results from the meteor detection algorithm.

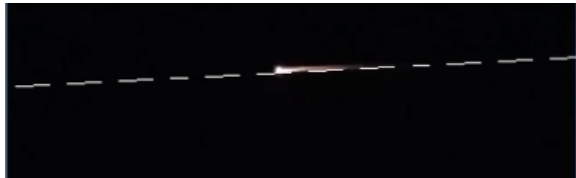


Figure 23: Detecting the meteor path



Figure 24: Detecting meteor blobs

DISCUSSION

The proposed mission concept will be a pathfinder for development of a constellation of CubeSats to detect meteor entry into the Earth’s atmosphere. Based on our preliminary design, we have shown that a mission may be accomplished using CubeSat components and technology. Two subsystems require further development and study to determine their implications on the proposed mission. This includes the propulsion system and autonomous meteor tracking system.

The propulsion system selected for RockSat is a Green Monoprop from Aerojet Rocketdyne. While this propulsion system has not been demonstrated in space, the design has been shown to work with hydrazine. The required delta-v is only 110 m/s and hence does not

stretch the capabilities of the Green Monoprop propulsion system.

The second subsystem of critical importance is the autonomous meteor tracking system. It is critical for this subsystem to operate nominally for us to achieve the primary mission objectives. A true test of the system can only be achieved during the demonstration. However, significant effort will be expended to develop simulation scenarios and simulated images/video to test the algorithm. Key challenges with the detection algorithm will be the signal to noise ratio achieved while in orbit and being able to distinguish and keep tracking the main object of reentry. As RockSat and the meteor re-enter the atmosphere, objects will come apart and it will be important for the tracking system to avoid focusing away from the minor objects falling/disintegrating.

Operating the two OSats will provide a taste of hosting many cameras from many viewpoints in space. The data streams from each satellite will be stitched together both for cross-correlation and for providing multiple views and insight of the composition of the meteor.

The ability to stitch or correlate image data from multiple-viewpoints and multiple satellites will provide a whole new capability in meteor entry and detection. Such an approach will help to simplify the detection problem and at times provide redundant data streams. This is where a network of satellites holds great potential.

CONCLUSIONS

In this paper, we have proposed the development of the Space Weather and Impact Monitoring Network (SWIMNet). SWIMNet will utilize two observer 3U CubeSats and a third, 6U CubeSat, carrying a 2 kg meteor that will reenter the Earth’s atmosphere. The observer satellites and ground telescope will be used to monitor the reentry event from multiple points of view and provide new and detailed insight into how a meteor reenters Earth’s atmosphere and breaks up. The observer satellite will be used to autonomously detect and track the reentry event. Beyond this demonstration, they will be used to track natural meteor reentry for up to a year. The proposed observer and meteor satellites can all be constructed using off-the-shelf CubeSat technology. Demonstration of this technology will pave a path forward towards development of a low-cost CubeSat or small satellite constellation to monitor meteor entry and provide time-critical warnings.

Acknowledgments

The authors would like to gratefully acknowledge the financial, technical and mentoring support of the

AFRL, AFOSR and the University NanoSatellite Program (UNP). The authors would like to also thank Prof. Vishnu Reddy from University of Arizona for technical mentorship of the meteor detection work.

References

1. S. Proud, (2013) "Reconstructing the orbit of the Chelyabinsk meteor using satellite observations," *Geophysics Research Letters*, Vol. 40, No. 13, pp.3351–3355.
2. V. Hernandez et al., "SWIMSat: Space Weather and Meteor Impact Monitoring using a Low-Cost 6U CubeSat," *Proceedings of the 30th Annual AIAA/USU Conference on Small Satellites*, Logan, UT, 2016.
3. G. S. Collins, J.H. Melosh, and R.A. Marcus, (2005), Earth Impact Effects Program: A Web-based computer program for calculating the regional environmental consequences of a meteoroid impact on Earth. *Meteoritics & Planetary Science*, 40: 817–840. doi:10.1111/j.1945-5100.2005.tb00157.x
4. M. Fries, J. Fries. (2010) "Doppler Weather Radar as Meteorite Recovery Tool, *Meteoritics and Planetary Science*," vol. 45, no. 9, pp. 1476–1487.
5. S. Miller, W. Straka III, A. Scott Bachmeier, T. Schmit, P. Partain, and Y. Noh. (2013) Earth-Viewing Satellite Perspectives on the Chelyabinsk Meteor Event, *Proceedings of the National Academy of Sciences*, Vol. 110, pp. 18092-18097.
6. W. A. Ailor, M. A. Weaver, "Reentry Breakup Recorder: An Innovative Device for Collecting Data During Breakup of Reentering Objects," *5th IAASS Conference A Safer Space for Safer World*, Noordwijk, Netherlands: European Space Agency, 2012.
7. A.T. Sidor, R. D. Braun, D. DePasquale, "RED-Data2 Commercial Reentry Recorder: Size Reduction and Improved Electronics Design," *AIAA Atmospheric Flight Mechanics Conference*, 2014.
8. M. Lin, T. Flatley, A. Geist, and D. Petrick. "NASA GSFC Development of the SpaceCube MINI." *Proceedings of the 25th Annual AIAA/USU Conference on Small Satellites*, Logan, Utah, 2011.